

Critical insights into the effect of shear on *in situ* reduction of graphene oxide in PVDF:
assessing by rheo-dielectric measurements

This content has been downloaded from IOPscience. Please scroll down to see the full text.

View [the table of contents for this issue](#), or go to the [journal homepage](#) for more

Download details:

IP Address: 130.130.221.32

This content was downloaded on 01/06/2016 at 14:25

Please note that [terms and conditions apply](#).

Materials Research Express



PAPER

Critical insights into the effect of shear on *in situ* reduction of graphene oxide in PVDF: assessing by rheo-dielectric measurements

RECEIVED
4 November 2015

REVISED
24 December 2015

ACCEPTED FOR PUBLICATION
13 January 2016

PUBLISHED
20 May 2016

Maya Sharma¹, Giridhar Madras² and Suryasarathi Bose³

¹ Center for Nano Science and Engineering, Indian Institute of Science, Bangalore-560012, India

² Department of Chemical Engineering, Indian Institute of Science, Bangalore-560012, India

³ Department of Materials Engineering, Indian Institute of Science, Bangalore-560012, India

E-mail: sbose@materials.iisc.ernet.in

Keywords: PVDF, graphene oxide, shear, rheology, rheo-dielectric

Abstract

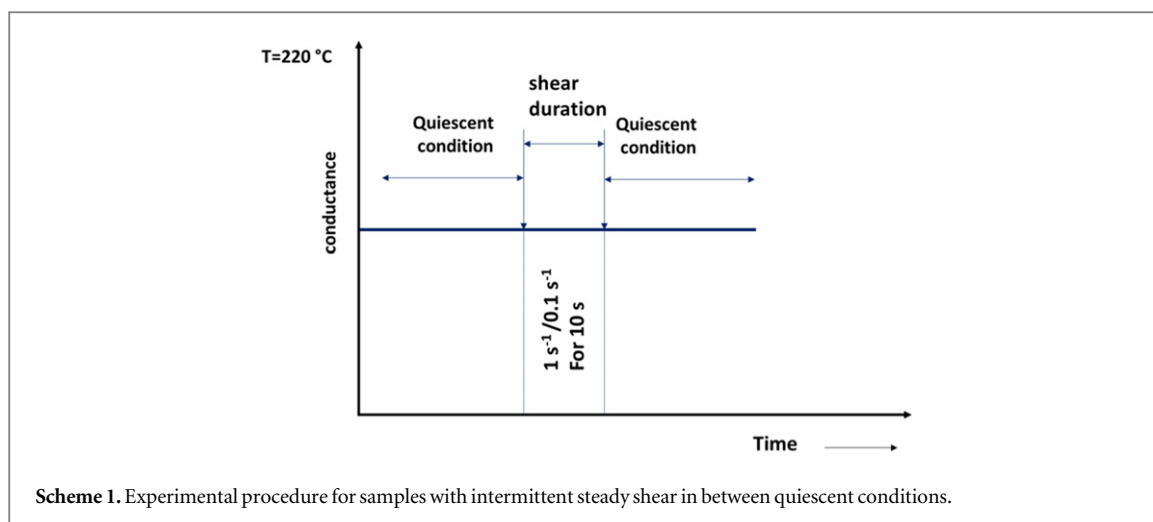
In situ reduction of graphene oxide (GO) during the preparation of conducting polymeric nanocomposites has been explored recently. In this study, the *in situ* reduction of GO in poly (vinylidene fluoride) (PVDF) under different conditions like quiescent, high and low shear, pre-shear has been investigated in detail. To accomplish this, PVDF/GO composites were prepared by both melt and solution blending. The bulk electrical conductivity of melt mixed composites, which had undergone extensive shear during preparation, was monitored by a rheo-dielectric setup and compared with the composites which experienced low shear. In addition, the bulk electric conductivity was also measured *in situ* for the composites that had undergone quiescent compositing. Comprehensive characterization of the composites reveals that GO is *in situ* reducing under all processes but the improvement in conductivity is dependent on the adopted process. Compression molded samples, which were annealed for 45 min, showed highest melt conductivity among all the adopted processes. The intense shearing of composites at high temperature in melt extrusion led to re-stacking of graphene sheets and resulted in decreased bulk electrical conductivity. Surprisingly, melt conductivity decreases with shear and time in all composites. This study can help in understanding the reduction of GO during intense shearing of composites.

1. Introduction

Graphene is considered to be superior to its other carbon counterparts due to its extraordinary intrinsic properties such as high specific surface area, chemical stability, optical transmittance and tunable band gap [1, 2]. The potential application of graphene varies from biotechnology [3] to high end electronics [4] supercapacitors [4], barrier coatings [5], solar cells [6], quantum electronics [7] and nanocomposite [8]. In addition, as a conducting nanocomposite [9, 10], the graphene sheets percolate to form a conductive mesh that can be used for various electrical or EMI shielding applications [11, 12].

The common method for the synthesis of graphene oxide (GO) is when the graphite crystals are first treated with acid that oxidizes the sheets introducing defects [13]. These defects help the layered graphite crystals to expand reducing the overall van der Waals forces and in exfoliation. The resulting compound can be further reduced to graphene (rGO) by thermal or by chemical reduction. Staudanmaier, Brodie and Hummers methods have been extensively used to produce the precursor of scalable graphene [13]. These methods use strong acids to introduce oxygen moieties such as the epoxy, hydroxyl or carboxyl groups [14, 15]. These defects disrupt the sp^2 hybridization thereby hindering the electron mobility of the π conjugated structure in graphene. Hence, GO is a poorly conducting material. Various strategies [16] such as thermal/chemical reduction, microwave assisted reduction [17], photocatalysis [14, 16, 18, 19] and *in situ* reduction of GO during processing of polymers have been used.

In our review article [20], we have extensively discussed various *in situ* methods to reduce GO in polymer during the composite preparation. The significance of *in situ* reduction of GO is that GO disperses



homogeneously into the polymer matrix compared to graphene and is then reduced to rGO that improves thermal and electrical conductivity of the polymer composite. Liu *et al* [21] reported the simultaneous dispersion and thermal reduction of GO during *in situ* melt polycondensation reaction of polymerization of terephthalic acid. Jin *et al* [22] employed a similar strategy to graft poly (butylene succinate) chains onto GO during *in situ* polymerization, resulting in rGO. The most common strategy for *in situ* reduction is the reduction of GO during compositing process. Various groups have adopted this strategy. For instance, Tang *et al* [23] used *in situ* reduction for reducing GO in poly (vinylidene fluoride) (PVDF) matrix and found improvement in conductivity by several orders, Ye *et al* [24] showed the flow-induced enhancement of *in situ* reduction of GO during the melt processing of polystyrene and observed high reduction of GO in the sheared melts compared to the quiescent melts. The *in situ* reduction of GO leads to homogeneous dispersion of reduced GO in polymer matrix resulting in good electrical and thermal properties at lower percolation thresholds. Thus the *in situ* reduction of GO is very promising from the processing point of view.

In this study, *in situ* reduction of GO in the sheared melt, in quiescent melt pressed under compression molding, and solution mixed PVDF/GO was comparatively investigated. The PVDF/GO composites obtained from different processes were systematically characterized by various techniques like Fourier transform infrared (FTIR), Raman and XPS. The effect of shear on the reduction of GO and on the conductivity was carefully studied. We believe that the results presented in this work will help in understanding the reduction of GO during shear in polymer matrix.

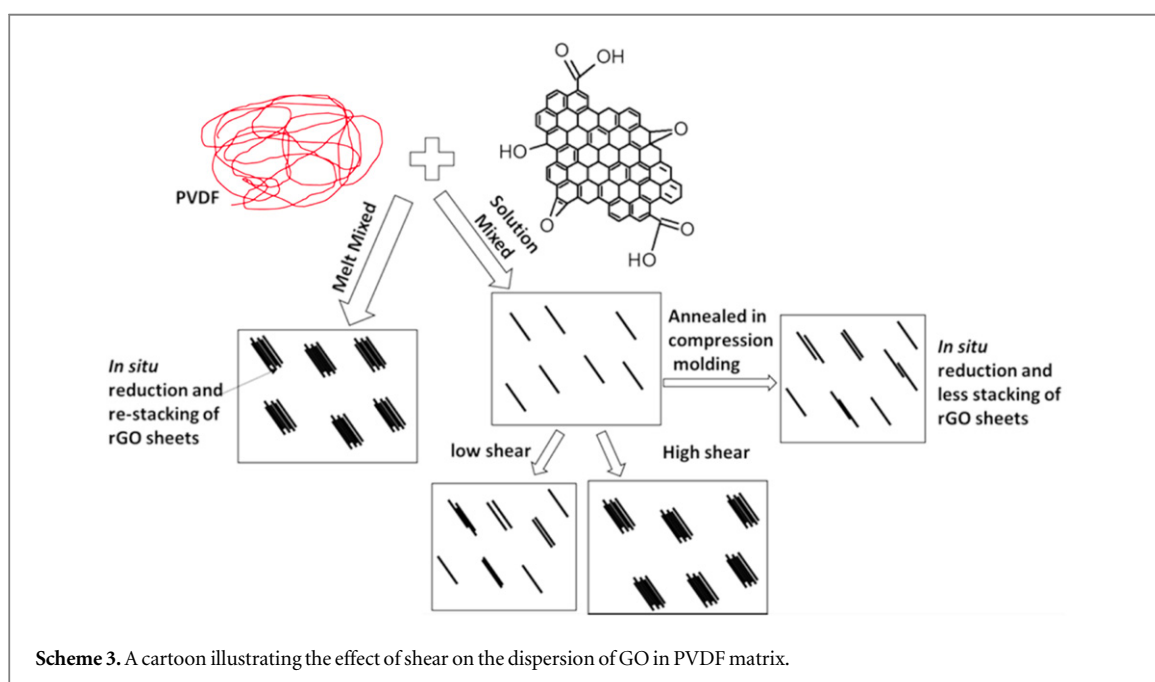
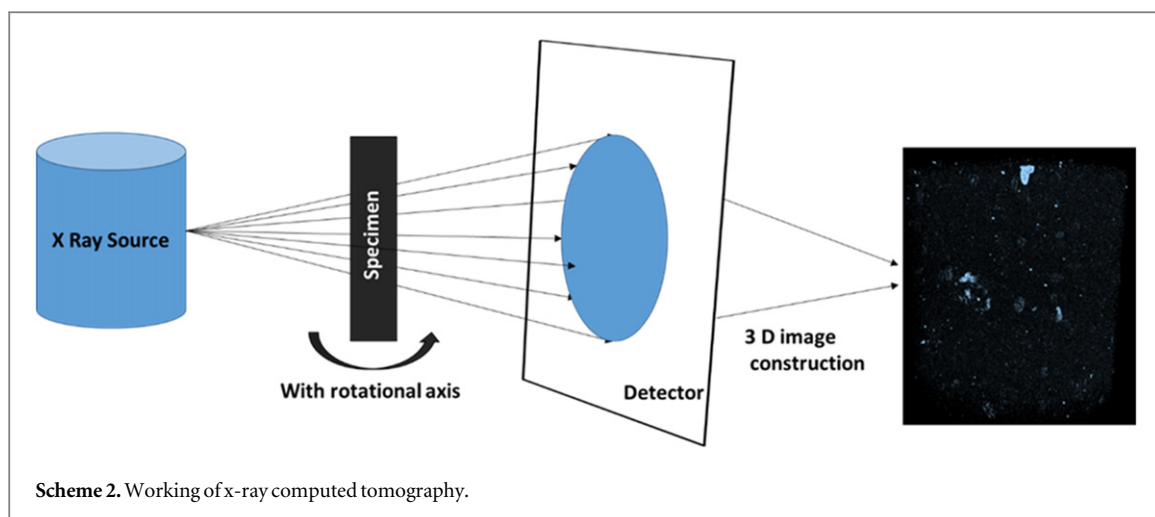
2. Experimental

2.1. Preparation of PVDF/GO composites

Commercial PVDF (Kynar-761 having M_w of 440 000 g mol⁻¹) was procured from Arkema Inc. (France). GO was synthesized by modified Hummer's method, as described earlier [25]. PVDF/GO composite was prepared by solution mixing. For solution mixing, GO (1, 2, 5 and 10 wt%) and PVDF were dispersed in DMF separately. PVDF solution and the dispersed GO solution were then mixed together using a shear mixer at 8000 rpm for 45 min. The PVDF/GO mixture was then poured into a glass petri dish and dried in vacuum oven. To realize the reduction of GO in the sheared melt, PVDF/GO composites (GO = 1, 2, 5 and 10 wt%) were prepared by melt blending (Haake, Mini lab II) at 220 °C at 60 rpm for 10 min in N₂ atmosphere. The effective shear rate inside a twin screw extruder was estimated to be nearly equal to the screw rate in rpm [26, 27].

To compare GO results with carbon nanotubes (CNTs), PVDF/CNT (2 wt%) composites was prepared using the same extruder conditions. Prior to melt mixing, both PVDF and GO were dried in a vacuum oven to remove moisture. To determine the reduction of GO in quiescent condition, the solution mixed composites were annealed in hydraulic press at 220 °C at 9 MPa for 45 min. The reduction of GO during rheology onto melt mixed samples was carried out using parallel plate DHR-3 (TA instruments) hybrid rheometer. The time dependent evolution of AC conductivity in the PVDF/GO composites before and after a steady shear rate was evaluated by rheo-dielectric set up. The rheo-dielectric set up consists of a special set of 25 mm parallel plates ring electrodes that are fitted with wiring and hardware for interfacing with a dielectric LCR meter (Agilent E4980A) that imposes a signal at a certain voltage and frequency

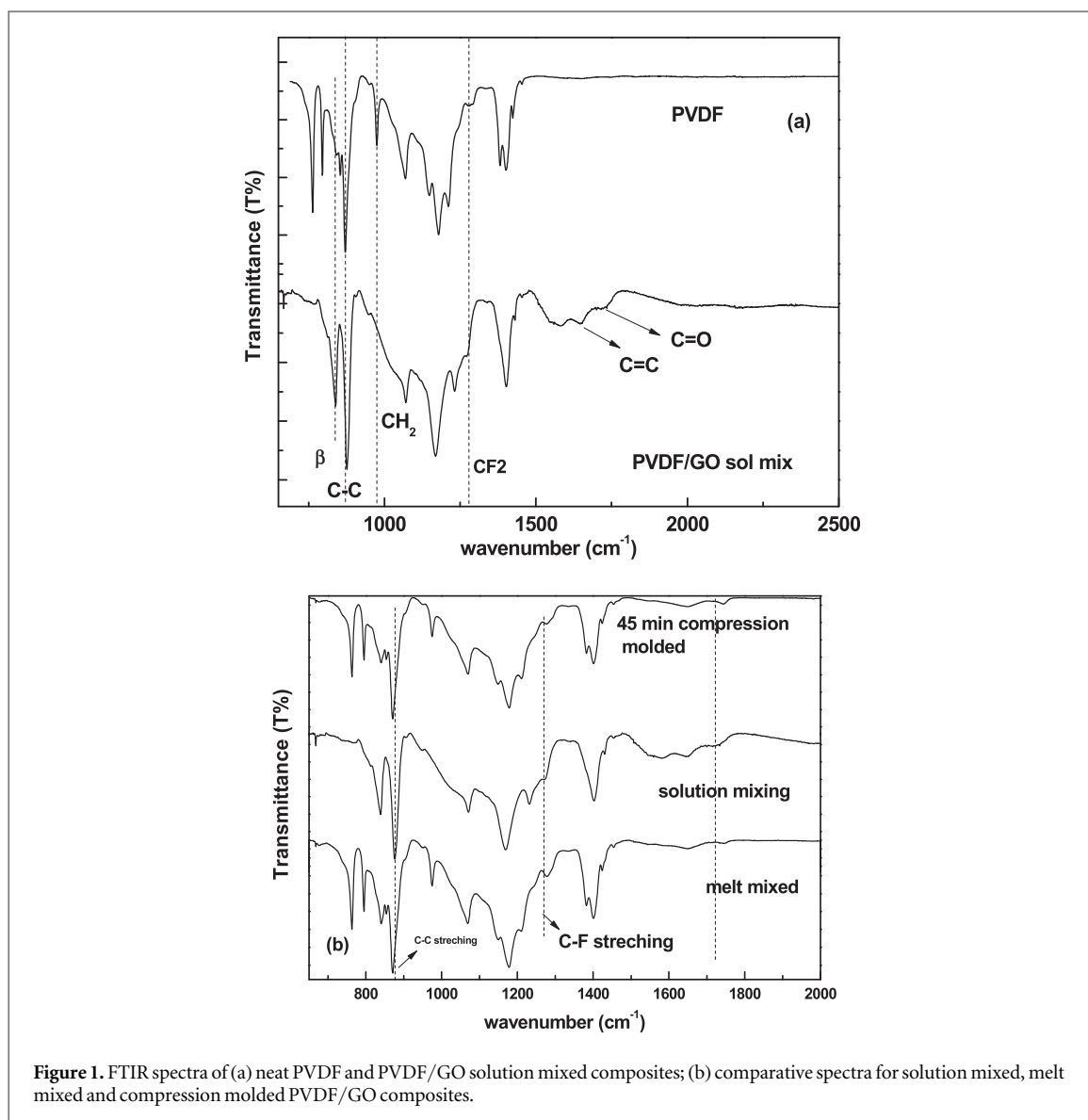
To study the reduction of GO during rheology, samples were melted at 220 °C and annealed under quiescent conditions. The experimental setup is shown in scheme 1. All the measurements were carried out under N₂



atmosphere to prevent oxidative degradation. As shown in scheme 1, the evolution of AC conductivity as a function of time was evaluated in three steps. In the first step, the samples were annealed for 30 min at 220 °C and the evolution of AC electrical conductivity was monitored. In the second step, an isothermal steady state shear rate was applied for 10 s. In the third step, the evolution of AC conductivity with respect to time after the applied shear rate was measured for 30 min. All experiments were performed in linear viscoelastic region and electrical measurements were carried out at constant frequency of 1 kHz. For comparison with PVDF/GO, PVDF/CNT (CNT ~ 2 wt%) was also prepared using melt extrusion with the same conditions as PVDF/GO composites.

2.2. Characterization

FTIR spectra of composite samples were recorded by a Perkin Elmer Frontier spectrophotometer using the ATR mode. XPS of composites were obtained using Kratos Analytical instrument. Raman spectra of composites were recorded on a micro LabRam spectrophotometer with 764 nm laser excitation. To investigate the morphology of the composites, 1 μm thick sections were prepared for light microscopy and for SEM with glass knives using an ultramicrotome (Leica EM UC 7). Morphological analysis was performed by means of a polarizing optical microscope using a 50 \times magnification objective. SEM (Zeiss) analysis was done by gold sputtering of composites. 3D micro computed tomography/microscopy (micro CT) of the composites was performed using Xradia 500 Versa. The scans were performed using 1100 projections over a 360° rotation using 60 kV voltage, 7 W power and 20 \times objective lens. Scheme 2 shows the working principle of micro CT.



2.3. Extraction of graphene based powder from composites

In order to indirectly determine the reduction and restacking of graphene sheets in composites, the graphene-based powders were isolated from the PVDF composites using solvent extraction. Typically, a few milligrams of PVDF composites were dissolved in DMSO under continuous stirring for few hours. Then the obtained dark black suspensions were centrifuged at 12 000 rpm for 30 min, and the supernatants were discarded. The extracted black powders were washed with DMSO to remove PVDF. The remaining precipitates were vacuum dried at $80\text{ }^\circ\text{C}$ for complete removal of moisture. The extracted powders were further characterized through Raman spectroscopy.

3. Results and discussion

3.1. Reduction of GO: assessing through FTIR, Raman and XPS

The solution mixed PVDF/GO composites are dark yellowish in color. After compression molding or melt mixing at $220\text{ }^\circ\text{C}$, the composites become black indicating the reduction of GO. This was further confirmed by spectroscopic techniques. FTIR is an effective tool to evaluate the reduction of GO and is shown in figures 1(a) and (b). From the FTIR spectra of neat PVDF (figure 1(a)), the characteristic peak at 763 cm^{-1} (CF_2 bending), 612 cm^{-1} (wagging mode of CF_2) and 976 cm^{-1} (twisting mode of CF_2) confirms the existence of α -phase. The characteristic peaks of GO corresponding to the oxygen-containing groups, i.e. the C=O carbonyl stretching [28] at 1720 cm^{-1} , stretching at 1647 cm^{-1} related to the vibrations of adsorbed water molecules [28, 29] etc are well evident in PVDF/GO samples (figure 1(a)). Interestingly, the PVDF/GO composite exhibited predominantly β -phase, which is manifested by a peak centered at 840 cm^{-1} . The transformation of α - to β -

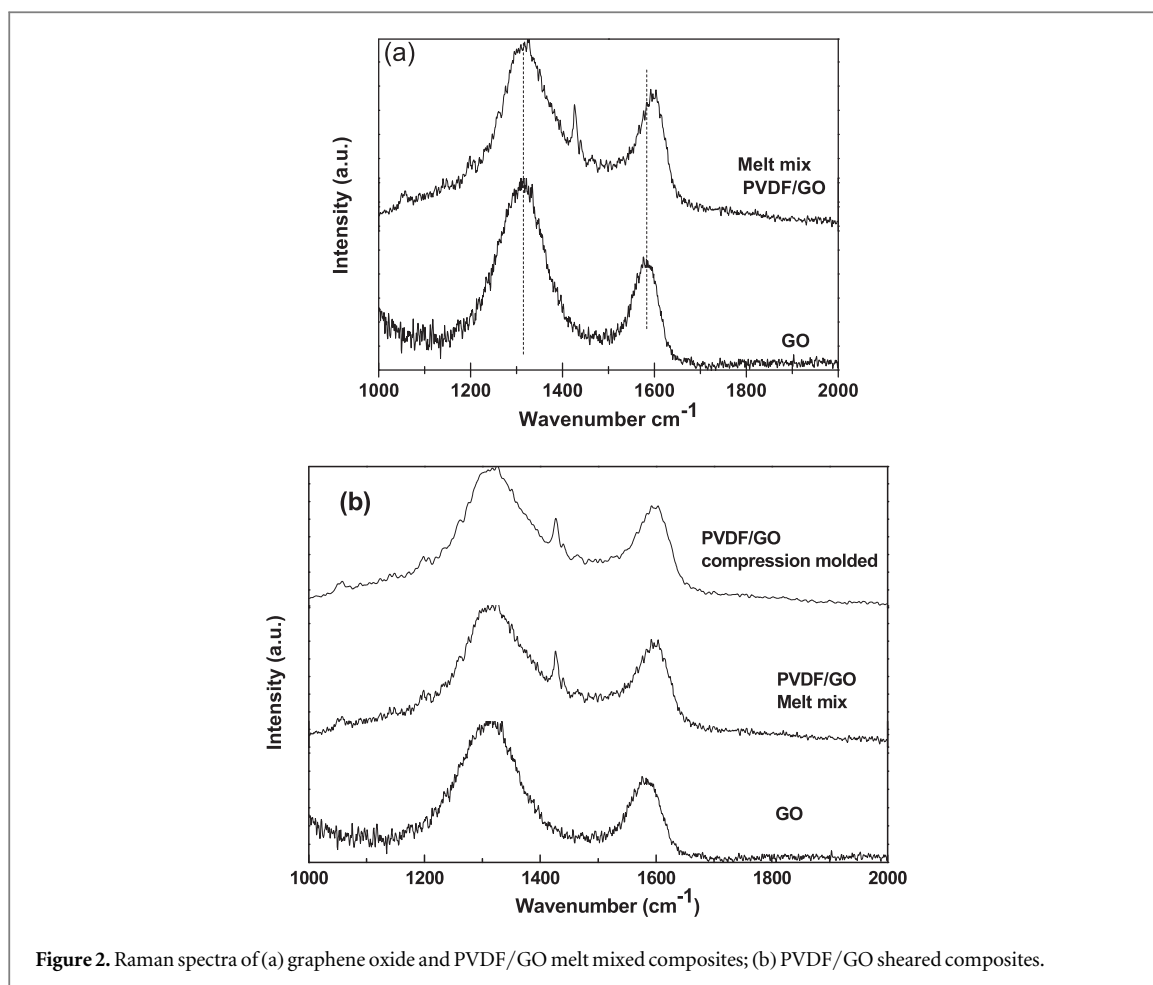


Figure 2. Raman spectra of (a) graphene oxide and PVDF/GO melt mixed composites; (b) PVDF/GO sheared composites.

phase is due to the specific interaction between fluorine group ($>CF_2$) of PVDF and carbonyl groups ($>C=O$) present on the GO surface.

In a recent article, we have reported the existence of predominantly β -phase in PVDF in the presence of 0.1 wt% GO [30]. The formation of the β -phase can be explained by the adsorption of PVDF chains onto GO sheets. This adsorption is strongly contingent on the interaction between PVDF chains and GO sheets. The adsorption of chains leads to the transformation of TGTG' (trans gauche) chains to TT (trans trans) conformation. The characteristic peak of C–C asymmetric stretching modes of PVDF/GO have shifted to 876 cm^{-1} in contrast to 871 cm^{-1} for neat PVDF. This can be attributed to specific interaction between GO and PVDF chains. Similarly, the C–F asymmetric vibrations of PVDF/GO shifted to 1271 cm^{-1} as compared to 1279 cm^{-1} in neat PVDF. This clearly confirms the dipole–dipole interaction between fluorine group ($>CF_2$) of PVDF and carbonyl groups ($>C=O$) present on the GO surface. However, in melt mixed and compression molded PVDF/GO composites, C–C asymmetric stretching modes of PVDF/GO is same as in neat PVDF (i.e. 871 cm^{-1}), whereas the C–F asymmetric vibrations of PVDF/GO have changed to 1277 cm^{-1} as against 1279 cm^{-1} in neat PVDF, as shown in figure 1(b). This indicates there is a favorable interaction between fluorine group of PVDF and carbonyl groups of GO. Interestingly, the absorbance intensity of carbonyl group ($>C=O$) is reduced in melt mixed and compression molded samples as compared to solution mixed samples. This indicates the reduction of GO to graphene in these processes. For instance, the $>C=O$ absorbance was 0.4280 for PVDF/GO solution mixed samples which decreased to 0.071 and 0.081 for melt mixed and compression molded samples, respectively. The C=O carbonyl stretching at 1720 cm^{-1} in PVDF/GO solution mixed samples has shifted to 1740 cm^{-1} in both melt mixed and compression molded samples. This can be attributed to specific interaction between GO and PVDF chains [30]. The shift in C=O stretching can possibly be due to interaction between PVDF and GO in compression molded and melt mixed composites [31].

Figure 2 illustrates the Raman spectra of GO and PVDF/GO melt mixed composites. In the spectrum corresponding to GO, the peaks at 1321 and 1582 cm^{-1} are well evident which corresponds to the D and G bands of graphene [31, 32]. In the composites, the G band shifted to higher wavenumber (i.e. 1599 cm^{-1}) while the D band remains in the same position. This upshift in the G band is mainly caused by charge doping with electron-withdrawing components of PVDF [33, 34]. Both FTIR and Raman spectra clearly indicate the interaction

Table 1. I_D/I_G ratio for different composites obtained from Raman spectra.

Sample	I_D/I_G
GO	1.18
PVDF/GO melt mix	1.25
45 min compression molded	1.39

between PVDF and GO sheets. The I_D/I_G ratios for all the composites are given in table 1. It is evident that I_D/I_G ratio increased for all composites as compared to the GO. This can be due to the reduction of GO to rGO during composite preparation. It is well documented that the relative strength of D band compared to G band is strongly contingent on the amount of disorder in the graphitic structure [35, 36].

During melt mixing, the composites are subjected to high shear and at high temperature where reduction of GO is facilitated. An increase of the edge planes, as well as the expansion of the disorder in the prepared reduced GO [31] can also be observed. It is very difficult to measure Raman spectra for solution mixed PVDF/GO composites due to the combined fluorescence from DMF, PVDF and GO [37]. Interestingly, PVDF/GO compression molded and all rheological sheared samples (discussed in subsequent sections) showed similar I_D/I_G ratio, which clearly indicates that compression molding for 45 min led to similar degree of reduction as in 10 min melt mixing of composites.

In order to understand the *in situ* reduction of GO under various processing conditions, XPS measurement were done, as shown in figures 3(a)–(c). XPS spectra in figure 3(a) show the C 1s signal of the PVDF/GO solution mixed composite. This signal was fitted by various oxygen containing components [37]: C=C and C–C (284.5 and 285.5 eV), C–H (286.3 eV), C=O (287.8 eV), O=C–OH (289.2 eV) and C–F at 290.8 eV. Based on our earlier studies [30], the C 1s carbon core structure of PVDF consists of a prominent peak at 285.87 eV which corresponds to C–H₂ species and the peak at 290.8 eV corresponds to C–F₂ species [38, 39]. In PVDF/GO composites (figure 3(a)), the –CH₂ peak is shifted to lower binding energy as compared to neat PVDF, which indicates that the –CH– bond is experiencing a strong interaction from highly electronegative oxygen. In melt mixed PVDF/GO composites, as shown in figure 3(b), the oxygen peak intensities in the C 1s peaks decrease significantly in comparison with those of PVDF/GO made by solution mixing. For instance, the peak that corresponds to C=O (287.8 eV) and O=C–OH (289.2 eV) decrease drastically with melt mixing. XPS results are in accordance with FTIR results, where C=O bond absorbance decrease drastically in melt mixed samples. These results clearly indicate the reduction of GO during melt mixing at 220 °C. Similar results were obtained for PVDF/GO compression molded samples (figure 3(c)). The –CH– peaks shifted to higher binding energy which indicated the decrease of oxygen environment in the vicinity. The C–C/O=C–OH group ratio for all the composites are given in table 2. It is evident that compression molded composites show high C–C/O=C–OH ratio than melt mixed and solution mixed composites. This can be ascribed to the reduction of GO to rGO during compression molding.

In summary, all three characterization techniques (FTIR, Raman and XPS) provide adequate evidence for the reduction of GO under melt mixed as well as in compression molded composites.

3.2. Effect of steady shear on the reduction of GO: assessing via rheo-dielectric

As one of the rationale behind this study is to examine the effect of steady shear on *in situ* reduction of GO, a parallel plate rheometer attached to a dielectric setup was employed to gain more insight. Figures 4(a)–(f) present time evolution of the AC conductivities of different PVDF/GO (with 1 and 5 wt% GO) composites during shear experiments (as explained in experimental section). Interestingly, we found that the compression molded (annealed for 45 min) composites show high AC conductivity than the melt mixed sample for both concentrations. For instance, initial conductivity for compression molded composite is ca $4 \times 10^{-4} \text{ S m}^{-1}$ (figure 4(c)), whereas the melt mixed sample showed an initial conductivity of ca $2 \times 10^{-5} \text{ S m}^{-1}$ (figure 4(e)). This suggests an efficient reduction of GO during annealing process. Another possible reason can be due to high shear present during melt mixing, restacking of reduced GO in the PVDF. This presumably leads to decrease in AC conductivity. Though in both conditions, the conductivity is decreasing with time and applied shear. The decrease in conductivity with time can be due to re-stacking of reduced GO due to strong van der Waals interactions between the sheets [40]. GO has specific interaction with PVDF, as observed from FTIR and XPS i.e. between the π electron cloud in graphene and high electron dense fluorine atoms in PVDF, it is very difficult to disperse GO sheets in PVDF.

To obtain a clear picture, we calculated the approximate shear applied during melt extrusion of composites. As mentioned in the experimental section, the melt mixing was done at 60 rpm at 220 °C for 10 min. In melt mixing, the estimated shear rate is ca 60 s^{-1} . This high shear rate for 10 min at 220 °C facilitates in the reduction

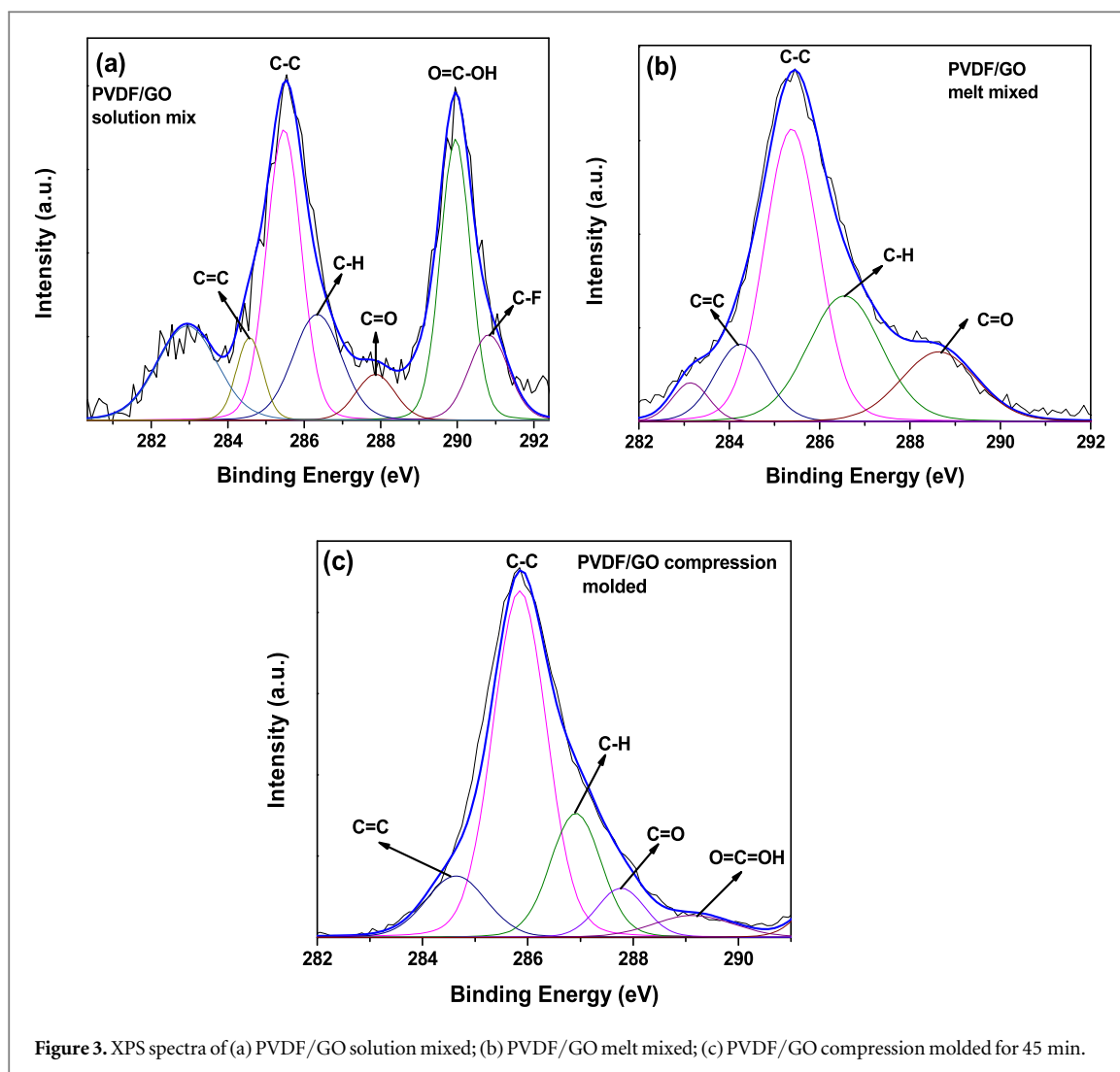


Figure 3. XPS spectra of (a) PVDF/GO solution mixed; (b) PVDF/GO melt mixed; (c) PVDF/GO compression molded for 45 min.

Table 2. C–C/O=C–OH ratio for different composites obtained from XPS spectra.

Sample	Ratio (C–C/ O=C–OH)
PVDF/GO solution mixing	1.13
PVDF/GO melt mixing	1.72
PVDF/GO compression molded annealed	2.96

of GO but at the same time results in re-stacking of reduced GO in PVDF that decreased the overall conductivity. To strengthen our hypothesis, we performed rheological experiments with solution mixed PVDF/GO samples (figure 4(d)). The AC conductivity of solution mixed samples is higher than melt mixed composites and moreover increases with time. This is similar to neat PVDF where conductivity increases with time. At $t \sim 1800$ s, a steady shear was applied. During this time, the AC conductivities decrease that indicates the destruction of conductive network paths. The recovery of DC conductivity takes place in solution mixed samples and tries to regain its conductivity. But after the second shear step, the conductivity does not recover which indicates the destructive effect of shear on the composites. This also denotes that, after shearing the composite for longer duration, dynamic percolation cannot be achieved in PVDF/GO composites. In an earlier work by Potschke *et al* [41], the PC/MWNTs composites showed similar destruction of network after first shear step. Similarly, in our earlier studies, in PC/SAN blend filled with MWNTs, the conductivity reduced marginally after shear and the MWNTs regains the percolating network leading to recovery of AC conductivity [42].

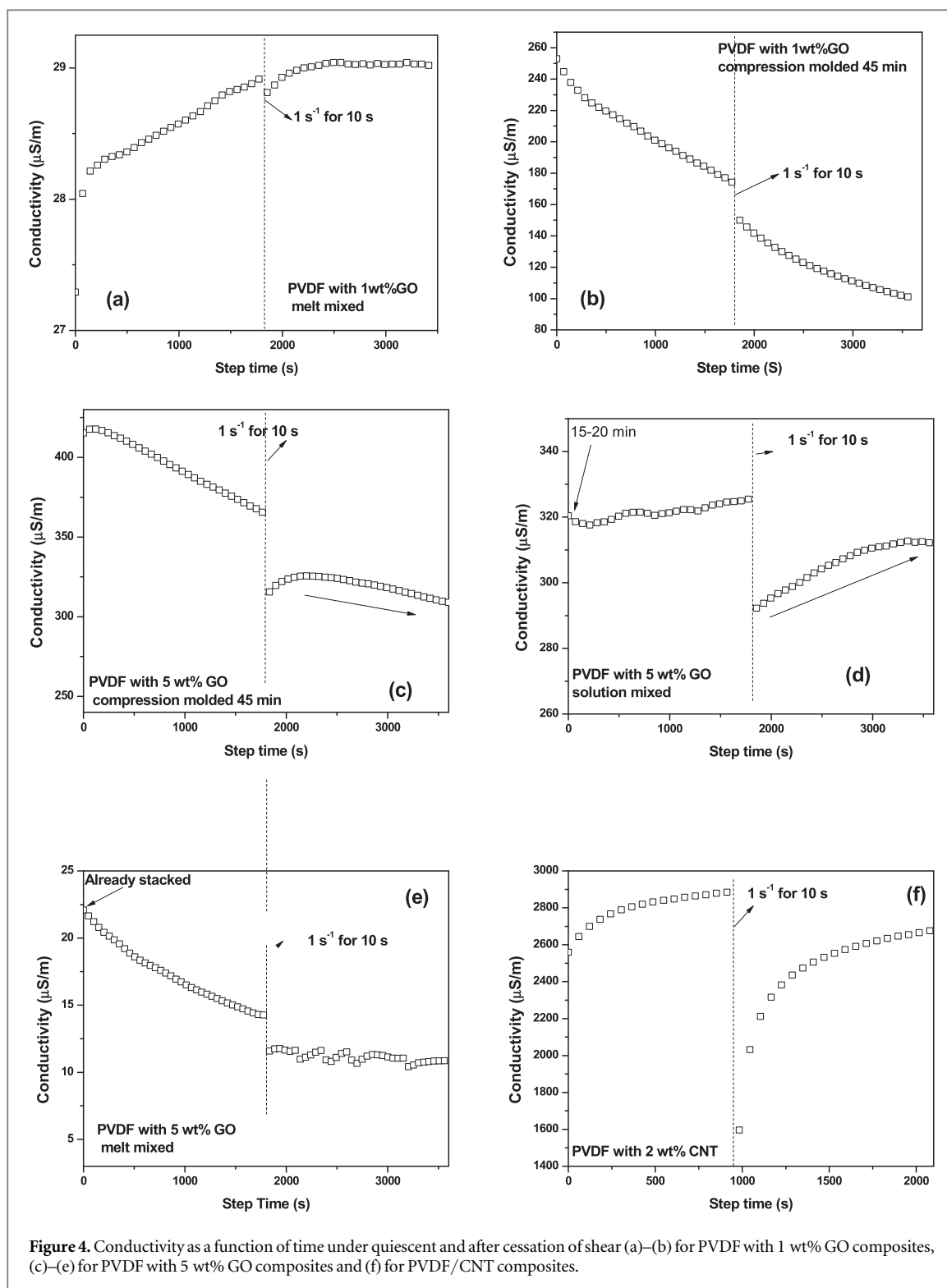


Figure 4. Conductivity as a function of time under quiescent and after cessation of shear (a)–(b) for PVDF with 1 wt% GO composites, (c)–(e) for PVDF with 5 wt% GO composites and (f) for PVDF/CNT composites.

However, in PVDF/GO composites show a contrasting effect, where conductivity continuously decreases even before and after cessation of shear.

Thus the conductivity of PVDF/GO composites is decreasing with shear and time irrespective of processing condition. Further, we tried to examine the effect of different shear rates and durations on the conductivity of composites. But, interestingly, the decrease in conductivity after cessation of shear is higher in compression molded and solution mixed samples as compared to melt mixed samples (figure 4). This implies the effect of shear duration of shear on the conductivity of samples. In melt extrusion, during mixing samples undergo high shear (i.e. ca. 60 s^{-1}) for 10 min, which leads to reduction of GO as well as restacking of GO in the matrix. Therefore, shear step in rheometer has no or little effect on the conductivity. In contrast, compression mold and

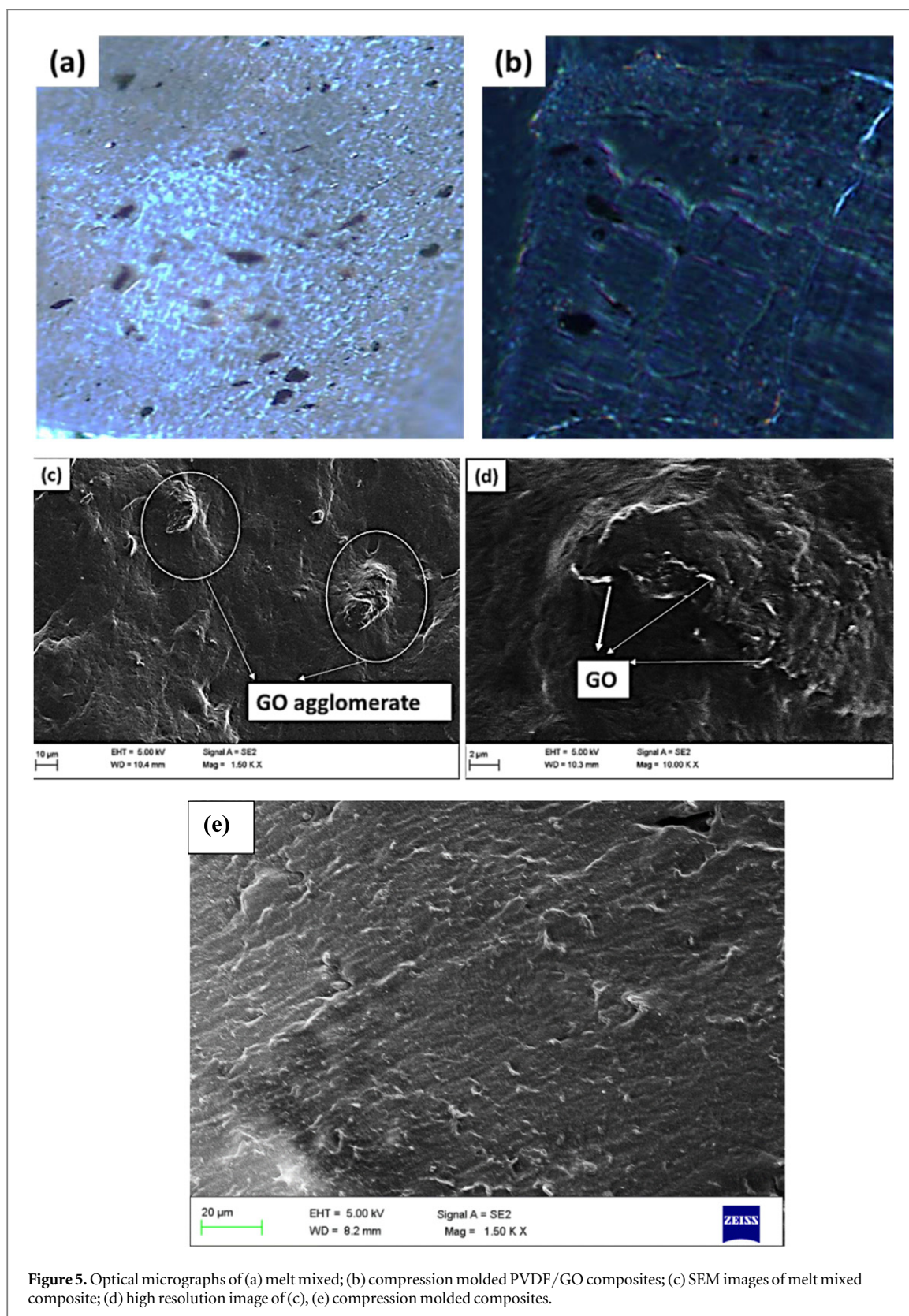


Figure 5. Optical micrographs of (a) melt mixed; (b) compression molded PVDF/GO composites; (c) SEM images of melt mixed composite; (d) high resolution image of (c), (e) compression molded composites.

solution mixed samples have not undergone any type of pre-shear during processing. Hence, the effect of shear is prominent in these composites.

The decrease in conductivity with time and shear is specific to GO based composites and different from CNT based composites. We prepared melt mixed PVDF/CNTs composites and applied shear step (1 s^{-1} for 10 s) between quiescent conditions (similar to PVDF/GO composites). The evolution of AC electrical conductivity was monitored, as shown in figure 4(f). The initial conductivity obtained was $2.6 \times 10^{-3} \text{ S cm}^{-1}$ which was

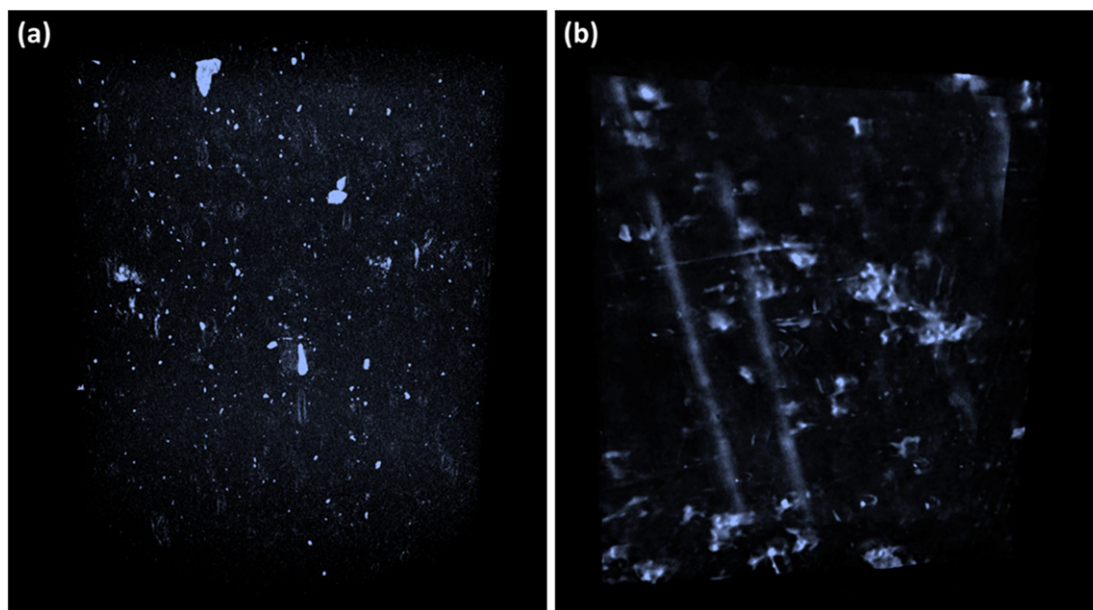


Figure 6. 3D constructed image of (a) compression molded sample, (b) melt mixed PVDF/GO nanocomposites.

further improved with time. At $t \sim 1800$ s, the shear step was applied. During this time, the DC conductivity decreases by some magnitude which indicates the destruction of conductive network paths. After a few minutes, the CNT network again starts percolating and DC conductivity recovered almost to the initial value [42, 43]. In CNTs based composites, the conductivity increases with annealing time and recovers to the initial position after shear cessation. In contrast, in GO based composites, the conductivity decreases with both time and shear.

Our hypothesis is that melt mixing leads to restacking of reduced GO in the PVDF matrix was further established by optical microscopy. Figures 5(a) and (b) show the optical micrographs of thin sections (ca $1 \mu\text{m}$) of composites. It is clearly evident that more restacking of rGO in melt mixed composites occurs as compared to compression molded composites. As more restacking is observed in melt mixed composites, this leads to decrease in conductivity that is in agreement with conductivity results. SEM micrographs of melt mixed composites are shown in figures 5(c)–(e). We can clearly observe that reduced GO restack in PVDF matrix, which deteriorate the percolating network of GO. Moreover, less stacking of rGO in compression molded composites as seen from in SEM micrographs in figure 5(e) is well evident.

Figure 6 shows the 3D re-constructed tomograms of (a) compression annealed and (b) melt mixed PVDF/GO nanocomposites. The white spots indicates GO as it scatters more than the low density polymer (PVDF). The dispersion of graphene is better in compression annealed composites as compared to melt mixed samples. As the concentration of GO is high in both the composites (i.e. 5 wt%), and graphene has tendency to agglomerate due to van der Waals' forces, it is difficult to comment on GO dispersion in these composites. However, we tried to locate GO in the composite using 3D micro CT and we got better dispersion of graphene in compression annealed samples. To further confirm this point, we measured AC conductivity of the composites (figure 7). As expected, PVDF with 5 wt% GO composites which were compression annealed for 45 min showed better conductivity than melt and solution mixed composites. These results are in accordance with SEM, Micro CT as well as rheo-dielectric measurements and supports better dispersion of graphene in compression annealed composites.

3.3. Characterization of the extracted graphene powders from composites

Raman spectra of extracted graphene powder are shown in figure 8. The 2D position of single-layer graphene sheets is usually observed to be at lower wavenumber than 2D band of multilayers [44]. The observed 2D bands of RGO in compression molded samples with a nearly symmetrical shape were centered at 2635 cm^{-1} , suggesting formation of few layered RGO sheets. While the shape of 2D bands of GO and solution mixed samples were similar with each other and the peak centered at 2662 cm^{-1} . This suggests that the solution mixed samples have not been greatly reduced whereas it is significantly reduced after compression.

In the current stage of the research, it is very crucial to understand the reduction of GO *in situ*. Although the extent of GO reduction during melt mixing and compression molding is similar, the morphology and properties of composites are very different. Melt mixing (high shear) leads to reduction of GO but altogether leads to

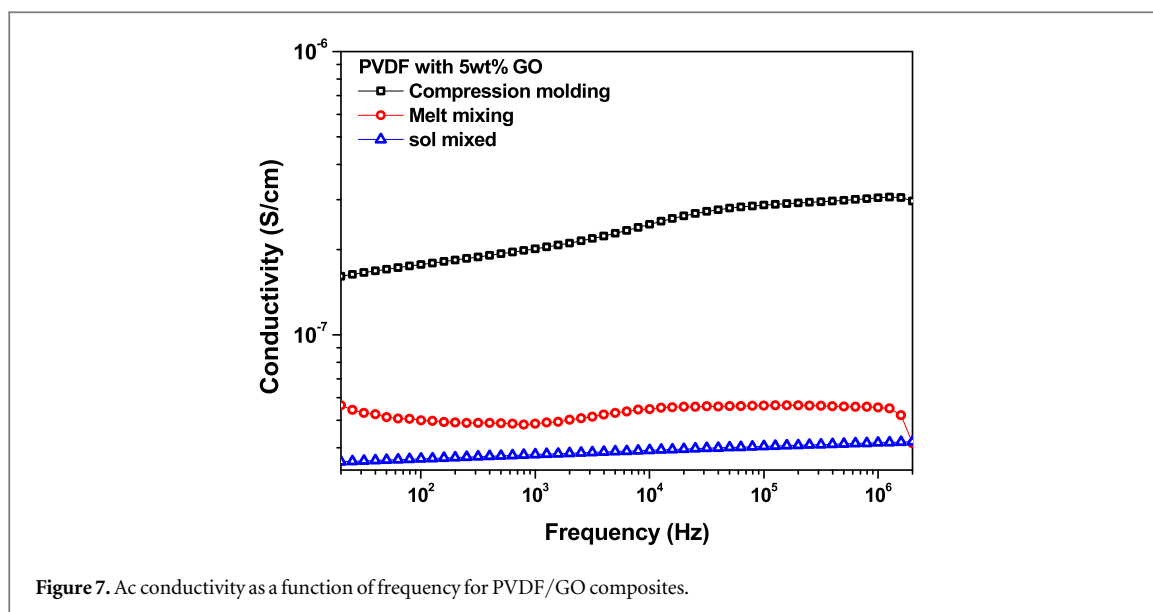


Figure 7. Ac conductivity as a function of frequency for PVDF/GO composites.

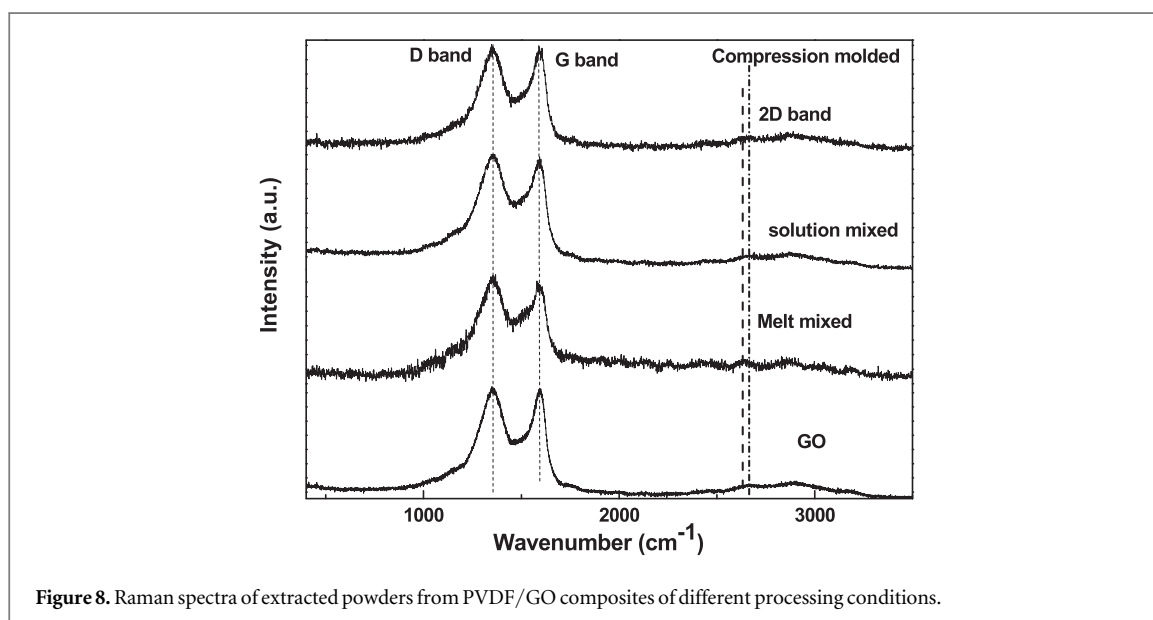


Figure 8. Raman spectra of extracted powders from PVDF/GO composites of different processing conditions.

restacking of graphene sheets which in turn reduces the bulk conductivity. Considering the great importance of melt blending for the preparation of polymer composites, further research is needed to understand the detailed mechanism.

4. Conclusions

In summary, we made a comparative study of *in situ* reduction of GO prepared by solution mixing, melt mixing, compression molded and melt mixing followed by rheological shearing. The comprehensive characterization of the composites indicates that the high temperature and shear leads to reduction of GO in polymer matrix but the improvement in conductivity is dependent on the adopted process. FTIR, Raman and XPS studies indicates that there is specific interaction between fluorine group of PVDF and carbonyl groups of GO. Interestingly, the absorbance intensity of carbonyl group ($>C=O$) is reduced in melt mixed and compression molded samples as compared to solution mixed samples, this indicates the reduction of GO to graphene in these processes. However, more restacking of rGO was observed in melt mixed composites as compared to compression-molded composites. As more restacking was observed in melt mixed composites, thus leads to decrease in conductivity, which is in agreement with conductivity results. A parallel plate rheometer attached to a dielectric setup was employed for melt conductivity. In all conditions, the conductivity is decreasing with time and applied shear.

The decrease in conductivity with time can be due to re-stacking of reduced GO, due to strong van der Waals interactions between the sheets. The compression molded showed high conductivity than melt mixed samples. This study can help in understanding the reduction of GO during intense shearing of composites.

Acknowledgments

Authors would like to acknowledge Department of Science and Technology (DST), India for their financial support. Authors would also like to acknowledge the MNCF facilities and staff at CeNSE, IISc.

References

- [1] Geim A K and Novoselov K S 2007 *Nat. Mater.* **6** 183–91
- [2] Rao C N R, Sood A K, Subrahmanyam K S and Govindaraj A 2009 *Angew. Chem., Int. Ed. Engl.* **48** 7752–77
- [3] Wang Y, Li Z, Wang J, Li J and Lin Y 2011 *Trends Biotechnol.* **29** 205–12
- [4] Wang Y, Shi Z, Huang Y, Ma Y, Wang C, Chen M and Chen Y 2009 *J. Phys. Chem. C* **113** 13103–7
- [5] Topsakal M, Şahin H and Ciraci S 2012 *Phys. Rev. B* **85** 155445
- [6] Wang X, Zhi L and Müllen K 2008 *Nano Lett.* **8** 323–7
- [7] Dragoman M and Dragoman D 2009 *Prog. Quantum Electron.* **33** 165–214
- [8] Kim H, Abdala A A and Macosko C W 2010 *Macromolecules* **43** 6515–30
- [9] Stankovich S, Dikin D A, Dommett G H, Kohlhaas K M, Zimney E J, Stach E A, Piner R D, Nguyen S T and Ruoff R S 2006 *Nature* **442** 282–6
- [10] Potts J R, Dreyer D R, Bielawski C W and Ruoff R S 2011 *Polymer* **52** 5–25
- [11] Liang J, Wang Y, Huang Y, Ma Y, Liu Z, Cai J, Zhang C, Gao H and Chen Y 2009 *Carbon* **47** 922–5
- [12] Pawar S P, Stephen S, Bose S and Mittal V 2015 *Phys. Chem. Chem. Phys.* **17** 14922–30
- [13] Hummers W S and Offeman R E 1958 *J. Am. Chem. Soc.* **80** 1339–39
- [14] Dreyer D R, Park S, Bielawski C W and Ruoff R S 2010 *Chem. Soc. Rev.* **39** 228–40
- [15] Unarunotai S, Murata Y, Chialvo C E, Mason N, Petrov I, Nuzzo R G, Moore J S and Rogers J A 2010 *Adv. Mater.* **22** 1072–7
- [16] Pei S and Cheng H-M 2012 *Carbon* **50** 3210–28
- [17] Zhu Y, Murali S, Stoller M D, Velamakanni A, Piner R D and Ruoff R S 2010 *Carbon* **48** 2118–22
- [18] Chua C K and Pumera M 2014 *Chem. Soc. Rev.* **43** 291–312
- [19] Dreyer D R, Ruoff R S and Bielawski C W 2010 *Angew. Chem., Int. Ed. Engl.* **49** 9336–44
- [20] Mural P K S, Sharma M, Madras G and Bose S 2015 *RSC Adv.* **5** 32078–87
- [21] Liu K, Chen L, Chen Y, Wu J, Zhang W, Chen F and Fu Q 2011 *J. Mater. Chem.* **21** 8612–7
- [22] Jin T-X, Liu C, Zhou M, Chai S-G, Chen F and Fu Q 2015 *Composites A* **68** 193–201
- [23] Tang H, Ehlert G J, Lin Y and Sodano H A 2011 *Nano Lett.* **12** 84–90
- [24] Ye S, Hu D, Zhang Q, Fan J, Chen B and Feng J 2014 *J. Phys. Chem. C* **118** 25718–24
- [25] Xavier P, Sharma K, Elayaraja K, Vasu K, Sood A and Bose S 2014 *RSC Adv.* **4** 12376–87
- [26] Dedecker K and Groeninckx G 1998 *Polymer* **39** 4993–5000
- [27] Wu S 1987 *Polym. Eng. Sci.* **27** 335–43
- [28] Loryuenyong V, Totepvimarn K, Eimburanaprat P, Boonchompoo W and Buasri A 2013 *Adv. Mater. Sci. Eng.* **2013** 5
- [29] Cao N and Zhang Y 2015 *J. Nanomaterials* **2015** 168125
- [30] Sharma M, Madras G and Bose S 2015 *Cryst. Growth Des.* **15** 3345–55
- [31] Ferrari A C et al 2006 *Phys. Rev. Lett.* **97** 187401
- [32] Zhu Y, Murali S, Cai W, Li X, Suk J W, Potts J R and Ruoff R S 2010 *Adv. Mater.* **22** 3906–24
- [33] Das B, Voggu R, Rout C S and Rao C N R 2008 *Chem. Commun.* 5155–7
- [34] Wang D, Bao Y, Zha J-W, Zhao J, Dang Z-M and Hu G-H 2012 *ACS Appl. Mater. Interface* **4** 6273–9
- [35] Wang Y y, Ni Z h, Yu T, Shen Z X, Wang H m, Wu Y H, Chen W and Shen Wee A T 2008 *J. Phys. Chem. C* **112** 10637–40
- [36] Fu C, Zhao G, Zhang H and Li S 2013 *Int. J. Electrochem. Sci.* **8** 6269–80
- [37] Shang J, Ma L, Li J, Ai W, Yu T and Gurzadyan G G 2012 *Sci. Rep.* **2** 792
- [38] Cho J S, Han S, Kim K H, Han Y G, Lee J H, Lee C S, Sung J W, Beag Y W and Koh S K 2005 Surface modification of polymers by ion-assisted reactions *Adhesion Aspects of Thin Films* vol 2 (Boca Raton, FL: CRC) pp 105–21
- [39] Ross G J, Watts J F, Hill M P and Morrissey P 2000 *Polymer* **41** 1685–96
- [40] Huang L, Lu C, Wang F and Wang L 2014 *RSC Adv.* **4** 45220–9
- [41] Alig I, Skipa T, Lellinger D and Pötschke P 2008 *Polymer* **49** 3524–32
- [42] Pawar S P, Pattabhi K and Bose S 2014 *RSC Adv.* **4** 18842–52
- [43] Pötschke P, Bhattacharyya A R and Janke A 2004 *Eur. Polym. J.* **40** 137–48
- [44] Shen J, Li T, Long Y, Shi M, Li N and Ye M 2012 *Carbon* **50** 2134–40